

High-Temperature, High-Pressure Hydrothermal Synthesis and Characterization of a Salt-Inclusion Mixed-Valence Uranium(V,VI) Silicate: $[\text{Na}_9\text{F}_2][(\text{U}^{\text{V}}\text{O}_2)(\text{U}^{\text{VI}}\text{O}_2)_2(\text{Si}_2\text{O}_7)_2]$

Yu-Chih Chang,[†] Wen-Jung Chang,[†] Sophie Boudin,[‡] and Kwang-Hwa Lii*,^{†,§}

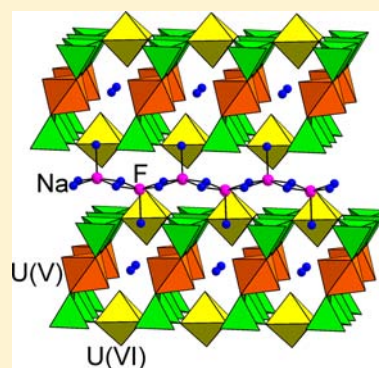
[†]Department of Chemistry, National Central University, Jhongli, Taiwan 320, Republic of China

[‡]Laboratoire CRISMAT, ENSICAEN, Université de Caen-Basse Normandie, 6 Bd Maréchal Juin, 14050 Caen Cedex, France

[§]Institute of Chemistry, Academia Sinica, Taipei, Taiwan 115, Republic of China

Supporting Information

ABSTRACT: A salt-inclusion mixed-valence uranium(V,VI) silicate, $[\text{Na}_9\text{F}_2][(\text{U}^{\text{V}}\text{O}_2)(\text{U}^{\text{VI}}\text{O}_2)_2(\text{Si}_2\text{O}_7)_2]$, was synthesized under hydrothermal conditions at 585 °C and 160 MPa and structurally characterized by powder and single-crystal X-ray diffraction (XRD). The valence states of uranium were established by U 4f X-ray photoelectron spectroscopy (XPS). The structure contains two-dimensional (2D) sheets of uranyl disilicate with the composition $[\text{UO}_2\text{Si}_2\text{O}_7]$, which are connected by $\text{U}(1)^{\text{V}}\text{O}_6$ tetragonal bipyramids to form thick layers. The Na^+ cations are located at sites in the intralayer and interlayer regions. In addition to Na^+ cations, the interlayer region also contains F^- anions such that infinite chains with the formula $\text{FNa}_{1/1}\text{Na}_{4/2}$ are formed. The same type of chain was observed in K_2SnO_3 . The title compound is not only the first example of salt-inclusion metal silicate synthesized under high-temperature, high-pressure hydrothermal conditions, as well as the first salt-inclusion mixed-valence uranium silicate, but it is also the first mixed-valence uranium(V,VI) silicate in the literature. Crystal data: $[\text{Na}_9\text{F}_2][(\text{U}^{\text{V}}\text{O}_2)(\text{U}^{\text{VI}}\text{O}_2)_2(\text{Si}_2\text{O}_7)_2]$, triclinic, $\text{P}\bar{1}$ (No. 2), $a = 5.789(1) \text{ \AA}$, $b = 7.423(2) \text{ \AA}$, $c = 12.092(2) \text{ \AA}$, $\alpha = 90.75(3)^\circ$, $\beta = 96.09(3)^\circ$, $\gamma = 90.90(3)^\circ$, $V = 516.5(2) \text{ \AA}^3$, $Z = 1$, $R_1 = 0.0241$, and $wR_2 = 0.0612$.



INTRODUCTION

Dissolved UO_2^{2+} , which is derived from the oxidative dissolution of uranium-bearing minerals, reacts with oxyanions to form relatively insoluble uranyl oxysalt minerals such as uranyl silicates, phosphates, vanadates, arsenates, and molybdates.¹ Uranyl silicates are the most abundant group of uranyl minerals, because of the ubiquity of dissolved silicon in most groundwaters. The crystal chemistry of uranyl silicates has been extensively studied, because an understanding of their structures is an important part of understanding the long-term performance of a geological repository for nuclear waste.² Recently, a large number of synthetic uranyl silicates and germanates, including an organically templated uranyl silicate, have been reported.³

We have been interested in the exploratory synthesis of new silicates and germanates of uranium with novel crystal structures and unusual oxidation states by high-temperature, high-pressure hydrothermal and flux-growth reactions. The chemistry of compounds containing uranium(V) is considerably less-developed, compared to the extensive catalogue of uranium(IV) and uranium(VI) compounds. Generally, uranium(V) in solution disproportionates to uranium(IV) and uranium(VI) rapidly, precluding the formation of uranium(V) compounds via hydrothermal synthesis. However, we have synthesized several uranium(V) silicates and germanates under high-temperature, high-pressure hydrothermal conditions.^{4a–c}

Although uranium(IV) is more common, few uranium(IV) silicates and germanates had been reported. Recently, we reported the first synthetic uranium(IV) silicate, $\text{Cs}_2\text{USi}_6\text{O}_{15}$, whose structure is closely related to that of $\text{Cs}_2\text{ThSi}_6\text{O}_{15}$ and those of several neodymium and zirconium silicates and germanates.^{4d} A uranium(IV) germanate that adopts a new structure and contains four- and five-coordinate germanium was also obtained: $\text{Cs}_4\text{UGe}_8\text{O}_{20}$.^{4e} In addition, several mixed-valence uranium silicates and germanates including uranium(IV,V), uranium(IV,VI), uranium(V,VI), and uranium(IV,V,VI) have been synthesized.^{4f–i} All mixed-valence uranium silicates and germanates with oxidation states of uranium from 4+ to 6+ have been observed.

Recently, we reported two salt-inclusion uranyl silicates, $[\text{K}_3\text{Cs}_4\text{F}][(\text{UO}_2)_3(\text{Si}_2\text{O}_7)_2]$ and $[\text{NaRb}_6\text{F}][(\text{UO}_2)_3(\text{Si}_2\text{O}_7)_2]$,⁵ which were synthesized at high temperature using a mixture of alkali-metal fluorides as fluxes. Previously, we had reported flux synthesis of $[\text{Na}_3\text{F}][\text{SnSi}_3\text{O}_9]$ and $[\text{K}_9\text{F}_2][\text{Ln}_3\text{Si}_{12}\text{O}_{32}]$ ($\text{Ln} = \text{Sm}, \text{Eu}, \text{Gd}$).^{6,7} In addition to silicates, many salt-inclusion phosphates, arsenates, oxalates, and vanadates have also been reported.⁸ These salt-inclusion compounds contain some extraordinary structural features. Structural studies have also revealed that the incorporated salts provide structure-directing

Received: April 7, 2013

Published: May 31, 2013

effects in the synthesis of noncentrosymmetric frameworks.⁹ Most of these compounds were synthesized by employing flux techniques at high temperature, and a few of them were prepared via a hydrothermal method at ~150 °C. During our continued exploratory synthesis of uranium silicates and germanates, we obtained a salt-inclusion mixed-valence uranium(V,VI) silicate, $[\text{Na}_9\text{F}_2][(\text{U}^{\text{V}}\text{O}_2)(\text{U}^{\text{VI}}\text{O}_2)_2(\text{Si}_2\text{O}_7)_2]$ (further denoted as **1**), under hydrothermal conditions at 585 °C and 160 MPa. It is not only the first example of salt-inclusion metal silicate synthesized under high-temperature, high-pressure hydrothermal conditions and the first salt-inclusion mixed-valence uranium silicate, but also the first uranium(V,VI) silicate reported in the literature. Herein, we report the synthesis, powder and single-crystal X-ray diffraction (XRD) study, and X-ray photoelectron spectroscopy (XPS) of **1**.

EXPERIMENTAL SECTION

Synthesis. High-temperature, high-pressure hydrothermal synthesis was performed using a Tem-Pres autoclave, where the pressure was provided by water. A reaction mixture of 203 μL of 10 M NaOH(aq), 42.6 mg of NaF, 58.1 mg of UO_3 , 57.7 mg of Na_2HPO_4 , and 203 μL of 10 M Na_2SiO_3 (aq) (the molar ratio of Na:F:U:P:Si = 39:5:1:2:10) in a 6.6-cm-long gold ampule (inner diameter = 0.48 cm) was placed in an autoclave and counterpressured with water at a fill level of 55%. The autoclave was heated at 585 °C for 2 d, cooled to 385 °C at 2 °C/h, and then rapidly cooled to room temperature via removal from the furnace. The pressure at 585 °C was estimated to be 160 MPa according to the pressure–temperature (P – T) phase diagram of pure water. The product was filtered, washed with water, rinsed with ethanol, and dried under ambient conditions. The reaction produced olive-green platelike crystals of **1**, together with a small amount of SiO_2 crystals and an unidentified colorless crystalline material. A qualitative energy-dispersive X-ray analysis of several olive-green crystals did not show any phosphorus and confirmed the presence of sodium, fluoride, uranium, and silicon. A suitable olive-green crystal was selected for single-crystal X-ray diffraction (XRD), from which the chemical formula was determined. These olive-green crystals were manually separated from the others, giving a pure sample as indicated by powder XRD. The yield of **1** was 71% based on uranium. Although hexavalent uranium reactant was used and no reducing agent was added in the reaction mixture, this reduced phase was obtained as a major product. Water could be the source of reduction under the high-temperature, high-pressure hydrothermal conditions. In this synthesis, although phosphate anion was not incorporated into the structure, it appears necessary for the formation of **1**. Under similar reaction conditions without Na_2HPO_4 , the major product was yellow crystals of Na_2USiO_6 .¹⁰

Single-Crystal X-ray Diffraction. An olive-green crystal of **1** having dimensions of 0.14 mm \times 0.06 mm \times 0.03 mm was selected for indexing and intensity data collection on a Bruker Kappa Apex II CCD diffractometer equipped with a normal focus, 3-kW sealed tube X-ray source. Intensity data were collected at 296 K over 1319 frames with φ and ω scans (width of 0.5°/frame) and an exposure time of 30 s/frame. Determination of integrated intensities and unit-cell refinement were performed using the SAINT program.¹¹ The SADABS program was used for absorption correction ($T_{\text{min}}/T_{\text{max}} = 0.478/0.746$).¹² On the basis of statistical analysis of intensity distribution and successful solution and refinement of the structure, the space group was determined to be $P\bar{1}$ (No. 2) with lattice constants of $a = 5.789(1)$ Å, $b = 7.423(2)$ Å, $c = 12.092(2)$ Å, $\alpha = 90.75(2)^\circ$, $\beta = 96.09(3)^\circ$, $\gamma = 90.90(3)^\circ$, and $V = 516.5(2)$ Å³. The structure was solved by direct methods and successive difference Fourier syntheses. One F and five Na atom sites were located and refined with full occupancy. The final cycles of least-squares refinement including atomic coordinates and anisotropic thermal parameters for all atoms converged at $R_1 = 0.0241$, $wR_2 = 0.0612$ for 1673 reflections with $I > 2\sigma(I)$, goodness of fit (Goof) = 1.110, $\rho_{\text{max}} = 1.21$ e Å⁻³ and $\rho_{\text{min}} = -1.58$ e Å⁻³. The large

value of the maximum and minimum main axis atom displacement parameter ratio for O(4), which is the bridging oxygen of disilicate group, may indicate unresolved disorder. All calculations were performed using the SHELXTL, version 6.14 software package.¹³ The crystallographic data are given in Table 1, and the selected bond distances are given in Table 2.

Table 1. Crystallographic Data for $[\text{Na}_9\text{F}_2][(\text{U}^{\text{V}}\text{O}_2)(\text{U}^{\text{VI}}\text{O}_2)_2(\text{Si}_2\text{O}_7)_2]$

parameter	value/comment
chemical formula	$\text{F}_2\text{Na}_9\text{O}_{20}\text{Si}_4\text{U}_3$
formula weight	1391.36
crystal system	triclinic
space group	$P\bar{1}$ (No. 2)
a [Å]	5.789(1)
b [Å]	7.423(2)
c [Å]	12.092(2)
α [°]	90.75(3)
β [°]	96.09(3)
γ [°]	90.90(3)
V [Å ³]	516.5(2)
Z	1
T [°C]	23
$\lambda(\text{Mo K}\alpha)$ [Å]	0.71073
D_{calc} [g cm ⁻³]	4.473
$\mu(\text{Mo K}\alpha)$ (mm ⁻¹)	23.99
R_1^a	0.0241
wR_2^b	0.0612

^a $R_1 = \sum ||F_o| - |F_c|| / \sum |F_o|$. ^b $wR_2 = [\sum w(F_o^2 - F_c^2)^2 / \sum w(F_o^2)^2]^{1/2}$, $w = 1/[\sigma^2(F_o^2) + (aP)^2 + bP]$, $P = [\text{Max}(F_o^2, 0) + 2(F_c^2)^2]/3$, where $a = 0.0223$ and $b = 2.76$.

Table 2. Selected Bond Lengths for $[\text{Na}_9\text{F}_2][(\text{U}^{\text{V}}\text{O}_2)(\text{U}^{\text{VI}}\text{O}_2)_2(\text{Si}_2\text{O}_7)_2]^a$

bond pair	bond length [Å]	bond pair	bond length [Å]
U(1)–O(1)	2.297(5) (2 \times)	U(1)–O(6)	2.352(5) (2 \times)
U(1)–O(8)	1.902(5) (2 \times)	U(2)–O(2)	2.231(5)
U(2)–O(3)	2.197(5)	U(2)–O(5)	2.191(5)
U(2)–O(7)	2.234(5)	U(2)–O(9)	1.860(6)
U(2)–O(10)	1.863(5)	Si(1)–O(1)	1.629(6)
Si(1)–O(2)	1.631(5)	Si(1)–O(3)	1.589(5)
Si(1)–O(4)	1.623(6)	Si(2)–O(4)	1.615(6)
Si(2)–O(5)	1.626(5)	Si(2)–O(6)	1.617(6)
Si(2)–O(7)	1.607(5)	F(1)–Na(2)	2.258(7)
F(1)–Na(4)	2.258(7)	F(1)–Na(4)	2.301(7)
F(1)–Na(5)	2.237(7)	F(1)–Na(5)	2.254(8)

^aNote that Na–O distances are available from the Supporting Information.

Powder X-ray Diffraction. In order to avoid oxidation or water intercalation through powder samples, selected olive-green crystals of **1** were ground in a glovebox under a nitrogen atmosphere, and the resulting powder was placed on a powder XRD sample holder and hermetically covered with a plastic thin film. The powder XRD pattern then was recorded using a Panalytical X'pert Pro X-ray diffractometer with a Cu K α source ($\lambda_{\text{av}} = 1.5418$ Å) for $2\theta = 5^\circ$ – 90° . The Rietveld refinement of the pattern was performed with the Fullprof Suite 2.05 software,¹⁴ based on the structure model of **1** determined from single-crystal XRD. The refinement of the cell, the profile, the preferred orientation parameters, and the background points led to values of $R_p = 12.1\%$, $R_{\text{wp}} = 16.4\%$, $R_{\text{bragg}} = 7.03\%$, and $R_t = 3.22\%$, indicating good agreement between the observed and calculated intensities. No impurity crystalline phase was detected. The observed, calculated

and difference powder XRD patterns are plotted in Figure 1. Details of the refinement in CIF format are available in the Supporting Information.

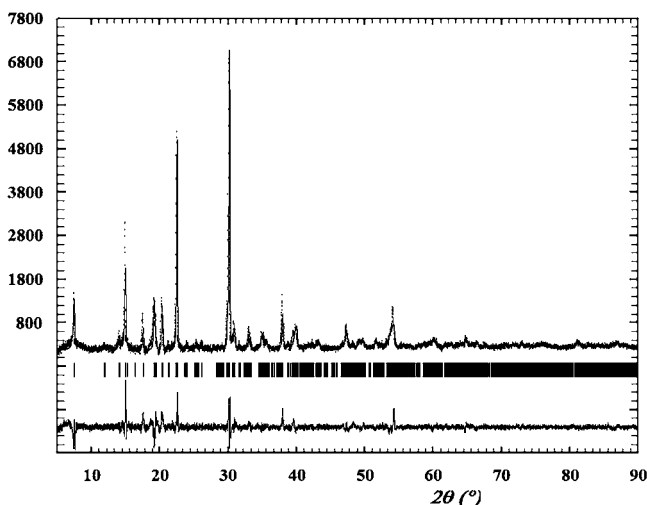


Figure 1. Experimental (dots), calculated (upper line), and difference (lower line) powder X-ray diffraction (XRD) patterns of **1**. The vertical bars indicate the positions of the Bragg reflections.

X-ray Photoelectron Spectroscopy (XPS). The XPS data on a crystal of **1** were recorded on a PHI Quantera SXM spectrometer using monochromatic Al K α (1486.6 eV) X-ray radiation at room temperature. The anode was operated at 24.2 W with a typical spot size of 100 μm . Argon ion sputtering was not applied. The binding energy scale was referenced to adventitious C 1s at 285.0 eV. The U 4f data were analyzed with MultiPak software using the iterated Shirley background and the asymmetric peak profile for both primary and satellite peaks.

RESULTS AND DISCUSSION

Structure. The structure of **1** consists of the following distinct structural elements: one Si_2O_7 unit, two UO_6 tetragonal bipyramids, one F, and five Na sites. U(1) and Na(1) are located at inversion centers, and all the other atoms are in general positions. Every SiO_4 tetrahedron shares a corner with another tetrahedron to form a Si_2O_7 unit, with the Si–O_{br}–Si bond angle at the bridging O atom, O(4), being 158.8(6)°. The Si–O_{br} bond length and Si–O_{br}–Si bond angle in **1** are in agreement with the correlation equation between the bond length $d(\text{Si–O}_{\text{br}})$ and the bond angle $\angle\text{Si–O}_{\text{br}}\text{–Si}$ for silicates given by Hill and Gibbs.¹⁵ The equivalent isotropic displacement parameter of O(4) is about twice of those for the other oxygen atoms, indicating positional disorder. The bridging O atom is disordered in directions at right angles to the Si...Si vector, as indicated by large U_{11} and U_{33} values. The U(1) O_6 tetragonal bipyramid has two short U–O bonds (1.902(5) Å (2X)) in trans positions and four longer U–O bonds (2.297(5)–2.352(5) Å) in the equatorial positions. The short U(1)–O bonds are significantly longer than the average U–O_{Ur} bond of 1.816 Å for $\text{U}^{6+}\phi_6$ tetragonal bipyramids in well-refined structures.² The sum of bond-valence incident at the U(1) site, calculated by using the bond-valence parameters $R_{ij} = 2.051$ Å and $b = 0.519$ Å for U, is 5.03 valence units, in accord with the occurrence of U^{5+} in this site.¹⁶ The four equatorial O atoms are shared with four SiO_4 tetrahedra belonging to two Si_2O_7 units, and the two apical O atoms are unshared. U(2) is bonded to six O atoms in a tetragonal bipyramid geometry with

two short U–O bonds (1.860(6) and 1.863(5) Å) in the uranyl unit, UO_2^{2+} , and four longer U–O bonds in the equatorial plane with bond lengths of 2.191(5)–2.234(5) Å. The bond-valence sum at the U(2) site, calculated with the parameters $R_{ij} = 2.074$ Å and $b = 0.554$ Å for $[\text{U}^{6+}]$ polyhedra, is 6.05 valence units.¹⁶ The four equatorial O atoms are shared with four different Si_2O_7 units, and the two uranyl O atoms are unshared.

As shown in Figure 2, each $\text{U(2)}^{\text{VI}}\text{O}_6$ tetragonal bipyramid shares four corners with four different Si_2O_7 units and each

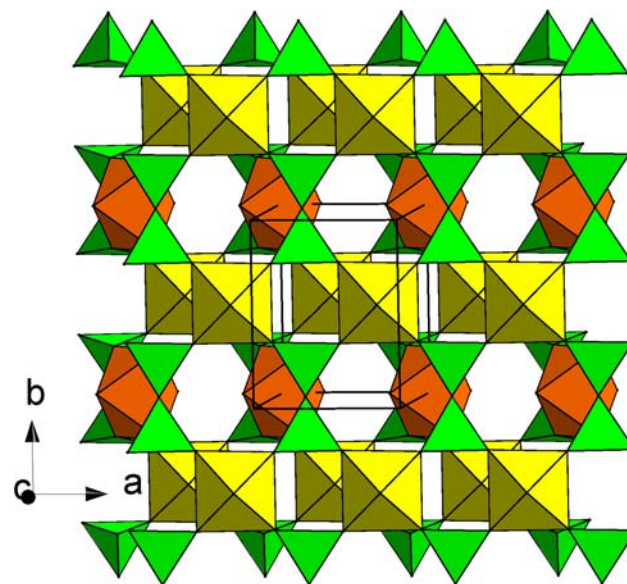


Figure 2. A layer in the structure of **1** viewed in a direction approximately parallel to the c -axis. Key: brown polyhedra, $\text{U(1)}^{\text{VO}}_6$; yellow polyhedra, $\text{U(2)}^{\text{VI}}\text{O}_6$; green tetrahedra, SiO_4 . Na and F atoms are not shown for the sake of clarity.

Si_2O_7 unit is connected to four $\text{U(2)}^{\text{VI}}\text{O}_6$ tetragonal bipyramids such that a 2D sheet of uranyl disilicate with the composition $[\text{UO}_2\text{Si}_2\text{O}_7]$ is formed. $\text{U(1)}^{\text{VO}}_6$ tetragonal bipyramids are located between two uranyl disilicate sheets and share two vertices with one disilicate unit from each sheet to form thick layers in the ab -plane. Within a layer, there are 8- and 7-ring channels parallel to the a - and b -axes, respectively (see Figure 3). The intralayer region contains Na(1)^+ and Na(3)^+ cations at the intersections of the channels. Adjacent layers are linked through bonds from the interlayer Na(2)^+ , Na(4)^+ , and Na(5)^+ cations to the O atoms of the uranyl silicate sheets. In addition to Na^+ cations, the interlayer region contains F^- anions. Each F atom is bonded to five Na atoms to form an FNa_5 square pyramid, which shares trans edges with two FNa_5 square pyramids to form an infinite chain with the formula $\text{FNa}_{1/1}\text{Na}_{4/2}$ (i.e., FNa_3) (see Figure 4). The apical Na atoms point alternately up and down along the chain. The chain is similar to that in the oxides K_2MO_3 ($M = \text{Zr}, \text{Sn}, \text{Pb}$), in which the 5-coordinate M(IV) atoms form the unusual MO_3 chains.¹⁷ It should be noted that the Na atoms are also bound to framework O atoms. On the basis of the maximum cation–anion distance by Donnay and Allmann,¹⁸ a limit of 3.19 Å was set for Na–O interactions, which gives the following coordination numbers: Na(1), 6-coordinate and bonded to O atoms only; Na(2), 8-coordinate, including one F atom at 2.258(7) Å; Na(3), 6-coordinate and bonded to O atoms only; Na(4), 6-coordinate, including two F atoms at 2.258(7) and 2.301(7) Å; Na(5), 6-coordinate, including two F atoms at

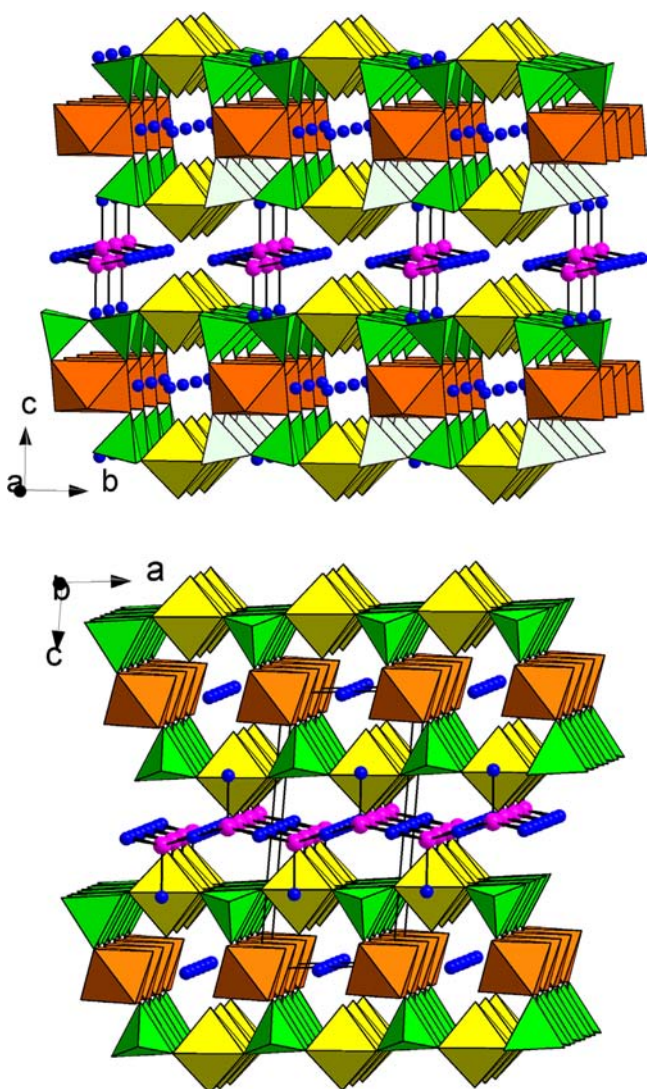


Figure 3. (Top) Polyhedral representation of the structure of **1** in a direction approximately parallel to the *a*-axis. Key: brown polyhedra, U(1)^VO₆; yellow polyhedra, U(2)^VO₆; green tetrahedra, SiO₄; purple circles, F atoms; blue circles, Na atoms. (Bottom) Structure of **1** viewed in a direction approximately parallel to the *b*-axis.

2.237(7) and 2.254(8) Å. The bond-valence sums for the Na⁺ cations are in the range of 0.87–1.01 valence units, and the sum for F(1) is 0.89.¹⁹ The bond-valence sums for all O atoms are close to 2.

Previously, we reported several uranium silicates and germanates containing uranium(V). Most of these compounds contain U^VO₆ octahedra sharing *trans* corners. Cs₃UGe₇O₁₈ was the only compound that contains discrete U^VO₆ octahedra.²⁰ Its room-temperature EPR spectrum can be simulated with two components using an axial model that are consistent with two distinct sites of uranium(V). We also reported a mixed-valence uranium(V,VI) germanate, A₃(U₂O₄)(Ge₂O₇) (A = Rb, Cs), whose structure consists of strings of UO₆ polyhedra sharing common corners to give infinite –U⁶⁺–O–U⁵⁺–O–U⁶⁺– chains.^{4f} Attempts to synthesize the silicate analogues were unsuccessful. Compound **1** is not only the first mixed-valence uranium(V,VI) silicate, but also the first silicate containing discrete U^VO₆ octahedra. It should also be noted that the U^VO₆ unit in **1** is considerably more distorted than those in the other uranium(V) silicates or germanates. For example, in the structure of Cs₃UGe₇O₁₈, the U(1)O₆ octahedron has a symmetry of S₆ with six equal U–O bond lengths of 2.148(3) Å, and the U(2)O₆ octahedron is slightly distorted with a symmetry of C₃ and U–O bond lengths of 2.114(3) Å (3×) and 2.147(3) Å (3×). In contrast, the U(1)^VO₆ unit in **1** has two short U–O bonds (1.902(5) Å (2×)) and four longer U–O bonds (2.297(5)–2.352(5) Å).

XPS Analysis. The U 4f XPS spectrum of **1** is shown in Figure 5, which is fitted with two components of U⁵⁺ and U⁶⁺. The fitting parameters of XPS data analysis are given in Table S1 in the Supporting Information. The binding energies (BEs) of all of the peaks were referenced to the adventitious C 1s at 285 eV. The BEs of U⁵⁺ were at 380.3 eV (U 4f_{7/2}) and 391.2 eV (U 4f_{5/2}), which are comparable to 380.2 and 391.1 eV of U⁵⁺ in Cs₃UGe₇O₁₈.²⁰ The BEs of U⁶⁺ were at 381.9 eV (U 4f_{7/2}) and 392.8 eV (U 4f_{5/2}), which are also comparable with those of U⁶⁺ compounds. For uranium, both the U 4f core-level peaks show shakeup satellites at higher BEs with the values of the separations, depending on the oxidation states of uranium. Typically, the separations are in the range of 6–7 eV for U⁴⁺, 7.8–8.5 eV for U⁵⁺, and 4 and 10 eV for U⁶⁺.²¹ The BEs of the satellites in **1** were at 388.9, 399.9, 385.8, 396.7, and 403.1 eV, from which the separations of the satellites from the main peaks

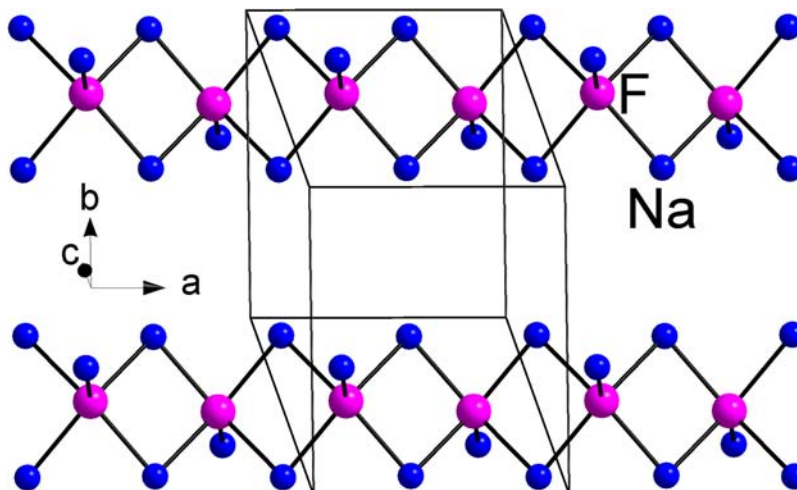


Figure 4. Two infinite chains formed of edge-sharing FNAs square pyramids in the structure of **1**.

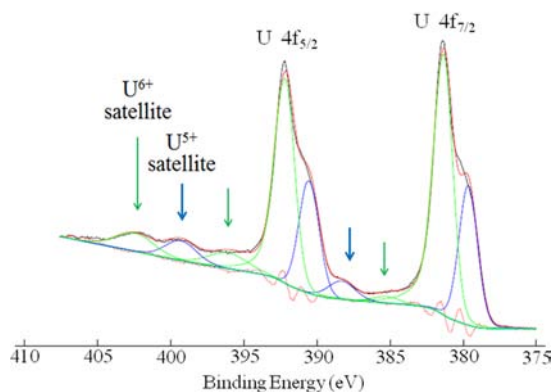


Figure 5. U 4f XPS spectrum of **1**. The spectrum is modeled with two components. [Solid black line represents experimental data; solid red line represents the fit envelope; solid blue line represents U^{5+} ; solid green line represents U^{6+} ; and dotted pink line represents the deviation.]

were 8.6 and 8.8 eV for the U^{5+} component, and 3.9, 3.9, and 10.3 eV for the U^{6+} component. The XPS spectrum of **1** indicates the presence of U^{5+} and U^{6+} with the main peak area ratio of 1.92 for U^{6+}/U^{5+} $4f_{7/2}$ and that of 2.01 for U^{6+}/U^{5+} $4f_{5/2}$. These values are in good agreement with the U^{6+}/U^{5+} ratio of 2:1 according to the results from crystal structure analysis.

CONCLUSION

In summary, we synthesized and characterized the first mixed-valence uranium(V,VI) silicate, $[Na_9F_2][(U^V O_2)(U^{VI} O_2)_2(Si_2 O_7)_2]$, which has a layer structure and contains Na^+ cations in the intralayer and interlayer regions. The interlayer region also contains F^- anions such that unusual infinite chains with the formula $FNa_{1/1}Na_{4/2}$ are formed. The valence states of uranium were established by U 4f X-ray photoelectron spectroscopy (XPS). It is not only the first example of salt-inclusion metal silicate synthesized under high-temperature, high-pressure hydrothermal conditions, but also the first salt-inclusion mixed-valence uranium silicate that has been reported in the literature. Most salt-inclusion compounds have been synthesized by employing flux techniques at high temperature, and a few of them have been prepared under mild hydrothermal conditions. The high-temperature, high-pressure method allows for new discoveries to be made through different metal salts and altered reaction conditions. Further research on the exploratory synthesis of more examples in this interesting system is in progress.

ASSOCIATED CONTENT

Supporting Information

The X-ray single-crystal crystallographic data of **1** in CIF format, the powder X-ray diffraction (XRD) data in CIF format, and X-ray photoelectron spectroscopy (XPS) fitting parameters. This material is available free of charge via the Internet at <http://pubs.acs.org>.

AUTHOR INFORMATION

Corresponding Author

*E-mail: liikh@cc.ncu.edu.tw.

Notes

The authors declare no competing financial interest.

ACKNOWLEDGMENTS

We thank the National Science Council of Taiwan for financial support and Ms. S.-L. Cheah at NTHU for XPS measurements.

REFERENCES

- (1) Finch, R.; Murakami, T. Systematics and Paragenesis of Uranium Minerals. In *Uranium: Mineralogy, Geochemistry and the Environment*; Burns, P. C., Finch, R., Eds.; Reviews in Mineralogy, Vol. 38; Mineralogical Society of America: Washington, DC, 1999; pp 91–179.
- (2) Burns, P. C. The Crystal Chemistry of Uranium. In *Uranium: Mineralogy, Geochemistry and the Environment*; Burns, P. C., Finch, R., Eds.; Reviews in Mineralogy, Vol. 38; Mineralogical Society of America: Washington, DC, 1999; pp 23–90.
- (3) (a) Wang, X.; Huang, J.; Liu, L.; Jacobson, A. J. *J. Mater. Chem.* **2002**, *12*, 406–410. (b) Chen, C.-S.; Kao, H.-M.; Lii, K.-H. *Inorg. Chem.* **2005**, *44*, 935–940. (c) Lin, C.-H.; Chiang, R.-K.; Lii, K.-H. *J. Am. Chem. Soc.* **2009**, *131*, 2068–2069. (d) Ling, J.; Morrison, J. M.; Ward, M.; Poinssatte-Jones, K.; Burns, P. C. *Inorg. Chem.* **2010**, *49*, 7123–7128. (e) Morrison, J. M.; Moore-Shay, L. J.; Burns, P. C. *Inorg. Chem.* **2011**, *50*, 2272–2277.
- (4) (a) Chen, C.-S.; Lee, S.-F.; Lii, K.-H. *J. Am. Chem. Soc.* **2005**, *127*, 12208–12209. (b) Lin, C.-H.; Chen, C.-S.; Shiryayev, A. A.; Zubavichus, Y. V.; Lii, K.-H. *Inorg. Chem.* **2008**, *47*, 4445–4447. (c) Nguyen, Q. B.; Chen, C.-L.; Chiang, Y.-W.; Lii, K.-H. *Inorg. Chem.* **2012**, *51*, 3879–3882. (d) Liu, H.-K.; Lii, K.-H. *Inorg. Chem.* **2011**, *50*, 5870–5872. (e) Nguyen, Q. B.; Lii, K.-H. *Inorg. Chem.* **2011**, *50*, 9936–9938. (f) Lin, C.-H.; Lii, K.-H. *Angew. Chem., Int. Ed.* **2008**, *47*, 8711–8713. (g) Lee, C.-S.; Wang, S.-L.; Lii, K.-H. *J. Am. Chem. Soc.* **2009**, *131*, 15116–15117. (h) Lee, C.-S.; Lin, C.-H.; Wang, S.-L.; Lii, K.-H. *Angew. Chem., Int. Ed.* **2010**, *49*, 4254–4256. (i) Nguyen, Q. B.; Liu, H.-K.; Chang, W.-J.; Lii, K.-H. *Inorg. Chem.* **2011**, *50*, 4241–4243.
- (5) Lee, C.-S.; Wang, S.-L.; Chen, Y.-H.; Lii, K.-H. *Inorg. Chem.* **2009**, *48*, 8357–8361.
- (6) Liao, C.-H.; Chang, P.-C.; Kao, H.-M.; Lii, K.-H. *Inorg. Chem.* **2005**, *44*, 9335–9339.
- (7) Tang, M.-F.; Chiang, P.-Y.; Su, Y.-F.; Jung, Y.-C.; Ho, G.-Y.; Chang, B.-C.; Lii, K.-H. *Inorg. Chem.* **2008**, *47*, 8985–8989.
- (8) (a) Huang, Q.; Ulutagay, M.; Michener, P. A.; Hwu, S.-J. *J. Am. Chem. Soc.* **1999**, *121*, 10323–10326. (b) Huang, Q.; Hwu, S.-J.; Mo, X. *Angew. Chem., Int. Ed.* **2001**, *40*, 1690–1693. (c) Hwu, S.-J.; Ulutagay-Kartin, M.; Clayhold, J. A.; Mackay, R.; Wardojo, T. A.; O'Connor, C. J.; Krawiec, M. *J. Am. Chem. Soc.* **2002**, *124*, 12404–12405. (d) Huang, Q.; Hwu, S.-J. *Inorg. Chem.* **2003**, *42*, 655–657. (e) Choudhury, A.; Dorhout, P. K. *Inorg. Chem.* **2006**, *45*, 5245–5247. (f) Queen, W. L.; West, J. P.; Hwu, S.-J.; VanDerveer, D. G.; Zarzyczny, M. C.; Pavlick, R. A. *Angew. Chem., Int. Ed.* **2008**, *47*, 3791–3794. (g) Vaidhyanathan, R.; Neeraj, S.; Prasad, P. A.; Natarajan, S.; Rao, C. N. R. *Angew. Chem., Int. Ed.* **2000**, *39*, 3470–3473. (h) Vaidhyanathan, R.; Natarajan, S.; Rao, C. N. R. *J. Solid State Chem.* **2002**, *167*, 274–281. (i) Vaidhyanathan, R.; Natarajan, S.; Rao, C. N. R. *Mater. Res. Bull.* **2003**, *38*, 477–483.
- (9) West, J. P.; Hwu, S.-J. *J. Solid State Chem.* **2012**, *195*, 101–107.
- (10) Shashkin, D. P.; Lure, E. A.; Belov, N. Y. *Sov. Phys. Crystallogr.* **1974**, *19*, 595–597.
- (11) Sheldrick, G. M. *SAINT, Version 7.68A*; University of Göttingen, Göttingen, Germany, 2009.
- (12) Sheldrick, G. M. *SADABS, Version 2008/1*; University of Göttingen, Göttingen, Germany, 2008.
- (13) Sheldrick, G. M. *SHELXTL Program, Version 6.14*; Bruker AXS GmbH: Karlsruhe, Germany, 2000.
- (14) Carvajal, J. R.; Roisnel, T. *Fullprof Suite Program, Version 2.05*; France, July 2011.
- (15) Hill, R. J.; Gibbs, G. V. *Acta Crystallogr., Sect. B: Struct. Crystallogr. Cryst. Chem.* **1979**, *B35*, 25–30.
- (16) Burns, P. C.; Ewing, R. C.; Hawthorne, F. C. *Can. Mineral.* **1997**, *35*, 1551–1570.
- (17) Gatehouse, B. M.; Lloyd, D. J. *J. Solid State Chem.* **1970**, *2*, 410–415.

- (18) Donnay, G.; Allmann, R. *Am. Mineral.* **1970**, *55*, 1003–1015.
- (19) Brown, I. D.; Altermatt, D. *Acta Crystallogr., Sect. B: Struct. Sci.* **1985**, *B41*, 244–247.
- (20) Nguyen, Q. B.; Chen, C.-L.; Chiang, Y.-W.; Lii, K.-H. *Inorg. Chem.* **2012**, *51*, 3879–3882.
- (21) Schindler, M.; Hawthorne, F. C.; Freund, M. S.; Burns, P. C. *Geochim. Cosmochim. Acta* **2009**, *73*, 2471–2487.